International Journal of Cardiology 282 (2019) 68–75

Contents lists available at ScienceDirect

International Journal of Cardiology

journal homepage: www.elsevier.com/locate/ijcard

Loss of Sox9 in cardiomyocytes delays the onset of cardiac hypertrophy and fibrosis

Antje Schauer *,[1], Volker Adams [1], David M. Poitz [1], Peggy Barthel [1], Dirk Joachim [1], Janet Friedrich [1], Axel Linke [1], Antje Augstein [1]

Department of Internal Medicine and Cardiology, University Hospital, TU Dresden, Germany

ARTICLE INFO

Article history:
Received 10 October 2018
Received in revised form 15 January 2019
Accepted 22 January 2019
Available online 2 February 2019

Keywords:
Sox9
TAC
Hypertrophy
Fibrosis

ABSTRACT

Background: The transcription factor Sox9 has been associated with cardiac injury and remodeling. Studies of mammalian hearts confirm Sox9 upregulation in fibroblasts following ischemic insults associated with enhanced fibrosis. The role of cardiomyocyte-specific Sox9 remains unclear. This study aimed to evaluate the role of cardiomyocyte-specific Sox9 in development and progression of left ventricular (LV) hypertrophy and fibrosis.
Methods: In male conditional Sox9 knockout mice (Sox9-KO) or floxed littermates (control group) transverse aortic constriction (TAC) was performed to induce LV hypertrophy. LV function and wall thickness were assessed weekly using echocardiography. LV mRNA- and protein expression levels of hypertrophy-, fibrosis-, and remodeling-associated genes were analyzed for each time point. Histological sections were stained for fibrosis and Sox9 expression.
Results: Only one week after TAC, the control group showed significantly enhanced heart weights and thickened LV posterior walls accompanied by elevated Anp- and Lox-mRNA levels. Simultaneously, Col1a1- and Col3a1-levels as well as Sox9 expression were strongly upregulated, Contrary, Sox9-KO mice did not develop cardiac hypertrophy until 4 weeks after TAC. Collagen and Sox9 expression also peaked at that later time point. Ejection fraction declined similarly in both groups after TAC. However, the control group showed a slightly better cardiac performance at 2 weeks after TAC.
Conclusions: Cardiomyocyte-specific Sox9 mediates hypertrophy and early fibrosis, following cardiac pressure-overload. Loss of Sox9 delays cardiac growth and remodeling processes, however, does not preserve the cardiac function. We suggest that cardiomyocyte-driven Sox9 initiates a pro-hypertrophic cascade, possibly involving a cross-talk between myocytes and fibroblasts.

1. Introduction

Cardiac stress induces structural and functional changes of the heart (remodeling) and finally leads to heart failure. Remodeling processes include the growth of cardiomyocytes (hypertrophy), which is accompanied by enhanced ANP synthesis [1,2] and interleukin-6 (Il-6) signaling [3], but also includes the loss of cardiomyocytes and increased accumulation of extracellular matrix (ECM, fibrosis) stiffening the ventricles and therefore impairing the myocardial function [4]. Studies on cardiac pressure-overload have identified lysyl oxidase (Lox) and matrix metalloproteinases (Mmp's), as promoting factors of cardiac hypertrophy, fibrosis and cardiac dysfunction [4–6]. Lox is synthesized and activated during myocardial stress and heart failure [7,8] mediating covalent collagen cross-linking between collagen type I and III, thereby increasing the collagen resistance to degradation by Mmp's. Since inhibition of Lox and Mmp2 resulted in preserved cardiac function, they have been introduced as potential therapeutic targets. However, upstream factors mediating their enhanced expression in response to cardiac stress are unclear.

The transcription factor Sox9 is an essential key player of chondrogenesis [9,10] and crucial for the correct formation of cardiac valves and septa [11–13]. Li et al. demonstrated Sox9 as a trigger of WNT5A expression, a crucial factor for embryonic heart development, and showed that attenuated binding of Sox9 favors cardiac malformations [14]. Besides its importance in the embryonic development, little is known about the role of Sox9 in health and disease of the adult mammalian heart. Several studies demonstrated that Sox9 is a negative regulator of chondrocyte calcification and required to prevent calcification in adult aortic valves [15–17]. Lacraz et al. found Sox9 to be a key player

* Corresponding author at: Technische Universität Dresden, Medizinische Fakultät, Labor fuer experimentelle und molekulare Kardiologie, Fetscherstr. 74, 01307 Dresden, Germany.
E-mail address: antje.schauer@tu-dresden.de (A. Schauer).
[1] This author takes responsibility for all aspects of the reliability and freedom from bias of the data presented and their discussed interpretation.

https://doi.org/10.1016/j.ijcard.2019.01.078
0167-5273/

of cardiac fibrosis following myocardial infarction in a mouse model [18]. They localized the activated transcription factor predominantly in cardiac fibroblasts repopulating the infarcted area after injury and reported a positive correlation with the expression of collagen type I. Beside the location in fibroblasts, Rahkonen et al. detected nucleus-located Sox9 in developing but also in adult murine cardiomyocytes [19].

To gain insight about a potential participation of cardiomyocyte-driven Sox9 during cardiac stress, we generated a cardiomyocyte-specific Sox9 knockout mouse and monitored hypertrophic and fibrotic processes within a murine model of pressure-overload.

2. Materials and methods

2.1. Mice

Cardiomyocyte-specific Sox9 knockout mice (KO) were obtained by crossing commercially available Sox9$^{flox/flox}$ mice (B6.129S7-Sox9^{tm2Crm}/J) and Myh6-cre mice (B6.FVB-Tg(Myh6-cre)2182Mds/J). Cre-negative littermates were used as control group (referred to as wildtype (WT)). In all experiments male mice, aged 12–16 weeks, were included. All mice were housed under standard conditions and maintained on normal mouse chow.

All procedures were licensed (DD24-5131/354/33) and carried out according to the institutional Animal Care guidelines as regulated by the German Federal law governing animal welfare.

2.2. Transverse aortic constriction (TAC)

TAC procedure was performed as described previously [20] using a blunted 27G cannula as spacer to create a standardized constriction of the aorta. Grade of stenosis was verified by measurement of the blood velocity in left and right carotic arteria by echocardiography. Sham operations were performed accordingly; however, instead of being knotted the suture was removed. Overall 169 animals underwent surgery, including 87 WT- and 82 KO mice. 4 WT- and 5 KO mice were excluded due to unsuccessful aortic banding. During the first week after TAC 17 WT mice and 15 KO mice died of post-operative complications, representing a comparable mortality rate of 18% and 19%, respectively.

2.3. Echocardiography

Mice were anesthetized by isoflurane and transthoracic echocardiography was performed using a Vevo3100 system (Visual Sonic, Fujifilm). B-Mode and M-Mode of parasternal long- and short axis were measured at the level of the papillary muscles. Heart function (LV ejection fraction (LVEF) and fractional shortening (FS)) were obtained using the Vevo LAB 2.1.0 software.

2.4. Immunohistochemistry

Paraffin-embedded heart sections (3 μm) were stained with hematoxylin-eosin (H&E), pricrosirius-red, Dapi (Sigma, 2,5 μg/ml), rabbit-polyclonal anti-Col4 (AB756P, Chemicon, 1:100), rabbit monoclonal anti-vimentin (2707-1, Epitomics, 1:100), rabbit polyclonal anti-troponin T2 (HPA015774, Sigma,1:100) and rabbit polyclonal anti-Sox9 (AB5535, Merck, Germany, 1:50) using standard protocols.

2.5. RNA isolation and quantitative real-time PCR

Total RNA was isolated from LV tissue using Qiazol reagent and miRNeasy Mini Kit (Qiagen, Germany) following standard protocols. cDNA was synthesized using Revert AID™ H Minus First Strand Synthesis Kit (Thermo Scientific, Germany) and oligo-dT primers. Real-time PCR was performed using the CFX96™ or CFX384™ Real Time PCR System (BioRad, USA) and Maxima SYBR Green qPCR Kit (Thermo Scientific, Germany). PCR program for all primer sets (Table 1; Supplementary material) were the following: 40 amplification cycles, each consisting of 95 °C for 10 s, 58 °C for 15 s and 72 °C for 30 s. Relative quantification of gene expression was calculated by $\Delta\Delta C_T$ method with Polr2a and Tbp as housekeeping genes using BioRad CFX Manager software (BioRad, USA).

2.6. Western blotting analysis

Isolation of proteins from QIAzol-lysed left ventricles (Qiagen, Germany) was performed by isopropanol precipitation following the standard protocol. Protein concentration was estimated with the BCA protein assay (Pierce, Thermo Scientific, Germany). Western Blots were performed using following antibodies: rabbit polyclonal anti-Sox9 (AB5535, Merck, Germany; 1:1000), rabbit polyclonal anti-Anp (PA5-29559, Thermo Scientific, Germany; 1:1000), rabbit monoclonal anti-cleaved Caspase 3 (cs9664, Cell signaling, Germany; 1:500) and mouse anti-β-actin (sc-47778, Santa Cruz, USA; 1:1000). Intensity of protein bands were estimated by the analysis software Vision-Capt (Vilber Lourmat, Germany) and normalized to β-actin.

2.7. Blinding and statistics

In all procedures of TAC surgery and echocardiography the operator was blinded to the mice genotype. For all statistical analyses SigmaPlot 12.5 was used. Data of the basic characterization of WT- and KO mice were analyzed by Student's *t*-test. Statistical analyses of TAC experiments were done using one-way ANOVA for comparison of data within each group and by two-way ANOVA for comparison of each time point between both groups. ANOVAs were followed by Holm-Sidak post hoc test. All data are expressed as mean ± SEM (standard error of the mean). p-Values below 0.05 were considered to be statistically significant.

3. Results

3.1. Animal characteristics

Due to the crucial role of Sox9 during embryonic development, full Sox9 KO (Sox9$^{-/-}$) mice are not viable and Sox9$^{+/-}$ mice die shortly after birth. That's why in vivo studies of Sox9 are limited to cell-specific KO models. We established a cardiomyocyte-specific Sox9 KO mouse, which is viable, reproductive and does not develop a pathological phenotype. Table 1 presents selected physiological parameters of KO and WT mice at the age of 12–16 weeks. Compared to WT, KO mice showed enhanced body- and heart weights. For further characterization, paraffin-embedded heart section areas were measured and revealed a non-significant tendency of enlarged heart areas in the KO group. Basic LV mRNA expression levels of Anp, Tgfβ-1 and Sox9 were slightly enhanced in the KO group indicating basal hypertrophic processes and a compensatory expression of Sox9 by non-cardiomyocytes.

3.2. Cardiac hypertrophy

We monitored the development of cardiac hypertrophy by echocardiography, measurement of heart weights and mRNA expression of hypertrophic markers (Anp, Bnp, Myh7 and Tgfβ-1 and -3) over a time

Table 1
Comparison of basic animal characteristics of untreated *Sox9$^{flox/flox}$*– and *Sox9$^{flox/flox}$*; *α-MHC-cre$^{+/-}$*-mice. Protein- and mRNA expressions levels were normalized to the housekeeping genes Polr2a and Tbp. mRNA- and protein values of the WT animals were normalized to 1. LV: left ventricle, RV: right ventricle, $n_{WT} = 7$, $n_{KO} = 7$.

	WT	*KO*	p-Value
	Mean ± SEM	Mean ± SEM	
Physiological data			
bodyweight [g]	27.38 ± 0.53	30.15 ± 1.22	0.06
Heart weight/tibia length [mg/mm]	7.55 ± 0.08	7.92 ± 0.08	0.01
Heart weight/body weight	4.84 ± 0.05	4.63 ± 0.13	0.25
Lung [wet weight/dry weight]	4.41 ± 0.06	4.37 ± 0.06	0.66
Histological data			
Area RV [mm^2]	1.39 ± 0.25	1.6 ± 0.25	0.59
Area LV [mm^2]	2.73 ± 0.3	3.06 ± 0.47	0.55
Overall heart area [mm^2]	14.53 ± 0.55	16.43 ± 1.04	0.11
Wall thickness [mm]	1.17 ± 0.05	1.28 ± 0.11	0.34
Wall thickness of septum [mm]	1.27 ± 0.09	1.23 ± 0.11	0.81
mRNA expression levels			
Anp	1.00 ± 0.13	2.04 ± 0.42	0.04
Bnp	1.00 ± 0.24	1.60 ± 0.22	0.10
Il-6	1.00 ± 0.09	1.16 ± 0.06	0.14
Myh7	1.00 ± 0.36	0.73 ± 0.14	0.49
Tgfβ-1	1.00 ± 0.05	1.31 ± 0.14	0.06
Tgfβ-3	1.00 ± 0.12	1.11 ± 0.15	0.57
Lox	1.00 ± 0.13	1.04 ± 0.17	0.85
Sox9	1.00 ± 0.09	1.23 ± 0.07	0.07
Col1a1	1.00 ± 0.16	1.32 ± 0.24	0.28
Col3a1	1.00 ± 0.23	1.17 ± 0.29	0.65
Fibronectin (Fn-1)	1.00 ± 0.08	1.11 ± 0.10	0.41
Protein expression levels			
Cleaved Caspase 3	1.00 ± 0.56	1.12 ± 0.69	0.89
ANP	1.00 ± 0.29	1.21 ± 0.19	0.55
Sox9	1.00 ± 0.13	1.17 ± 0.14	0.22

period of 4 weeks after TAC. While the heart weight of WT mice was significantly enhanced already one week after TAC, KO mice did not develop significantly enhanced heart weights until four weeks after TAC (Fig. 1A). In the WT group the diameter of the LV posterior wall (LVPW, Fig. 1B) as well as the cardiomyocyte diameter (Fig. 1D, E) steadily increased over the entire time period while no significant

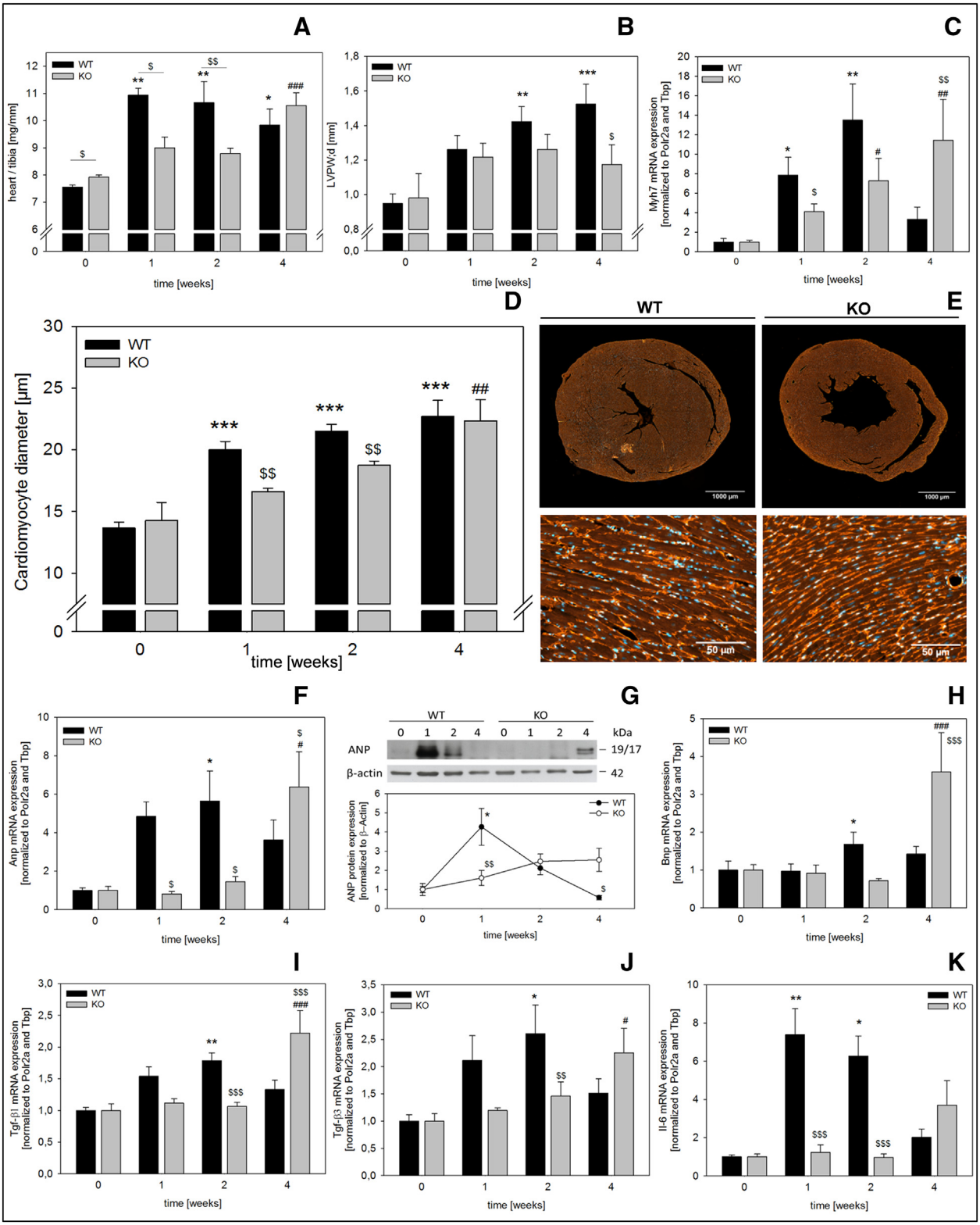

Fig. 1. Comparison of cardiac hypertrophic responses of WT- and KO mice during pressure-overload. Heart/tibia ratio (A), LVPW (B), LV mRNA expression of Myh7 (C). Diameters of cardiomyocytes (D) were measured in Collagen IV-stained heart sections (E). Fluorescence pictures show representative heart sections of WT- (left) and KO mice (right) after 2 weeks of pressure-overload. LV expression of Anp on mRNA (F) and on protein level (G), LV mRNA expression of Bnp (H), TGF-β1 (I), TGF-β3 (J) and Il-6 (K). n = 8–12. Time point 0 presents data before the intervention. For measurement of mRNA- and protein expression time point 0 was set to 1 for WT and KO, respectively. All data were expressed as mean ± SEM. $^{*}p < 0.05$ vs. WT_{0weeks}; $^{**}p < 0.01$ vs. WT_{0weeks}; $^{***}p < 0.001$ vs. WT_{0weeks}; $^{\#}p < 0.05$ vs. KO_{0weeks}; $^{\#\#}p < 0.01$ vs. KO_{0weeks}; $^{\#\#\#}p < 0.001$ vs. KO_{0weeks}; $^{\$}p < 0.05$ vs. $WT_{same\ time\ point}$; $^{\$\$}p < 0.01$ vs. $WT_{same\ time\ point}$; $^{\$\$\$}p < 0.001$ vs. $WT_{same\ time\ point}$.

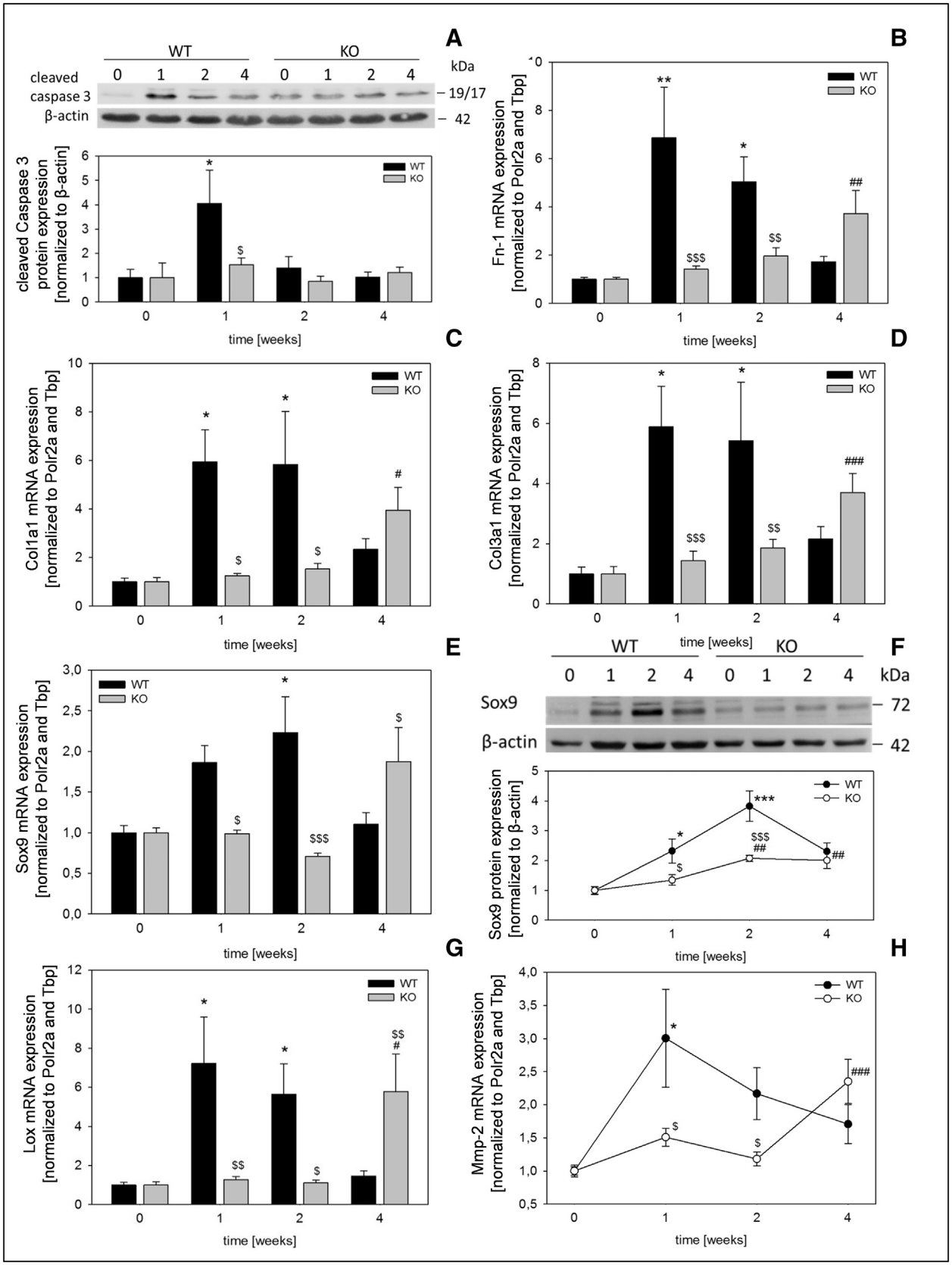

Fig. 2. Comparison of cardiac apoptotic and fibrotic processes of WT- and KO mice during pressure-overload. LV protein expression of cleaved Caspase 3 (A), LV mRNA expression of Fn-1 (B), Col1a1 (C), Col3a1 (D), LV expression of Sox9 on mRNA- (E) and protein level (F), Lox (G) and Mmp-2 (H). n = 7–12. Time point 0 presents data before the intervention. For measurement of mRNA- and protein expression time point 0 was set to 1 for WT and KO, respectively. All data were expressed as mean ± SEM. $^{*}p < 0.05$ vs. WT_{0weeks}; $^{**}p < 0.01$ vs. WT_{0weeks}; $^{***}p < 0.001$ vs. WT_{0weeks}; $^{\#}p < 0.05$ vs. KO_{0weeks}; $^{\#\#}p < 0.01$ vs. KO_{0weeks}; $^{\#\#\#}p < 0.001$ vs. KO_{0weeks}; $^{\$}p < 0.05$ vs. $WT_{same\ time\ point}$; $^{\$\$}p < 0.01$ vs. $WT_{same\ time\ point}$; $^{\$\$\$}p < 0.001$ vs. $WT_{same\ time\ point}$.

increase of LVPW was observed in the KO group. Accordingly, expression levels of Myh7 (Fig. 1C), Anp (Fig. 1F, G), Bnp (Fig. 1H) and Tgfβ-1 and -3 (Fig. 1I, J) were enhanced in WT mice and peaked at 2 weeks of pressure-overload but not until week 4 of TAC in KO hearts. Since enhanced expression of the cytokine Il-6 has been reported to be associated with hypertrophic growth LV mRNA expression levels of Il-6 were analyzed and revealed an almost 8-fold higher expression after one week of pressure-overload in WT mice (Fig. 1K). Contrary, in KO mice no enhanced Il-6 levels were observed until 4 weeks after TAC.

No signs for cardiac hypertrophy were measured after 4 weeks of sham operation (data not shown). Also LV function and mRNA expression levels did not differ from data of untreated WT and KO animals, respectively. Therefore, and to minimize animal suffering according to the 3R rule (reduction), in all subsequent analyses we just focused on a comparison between WT and KO at different time points after TAC.

3.3. Apoptosis and fibrosis during pressure-overload

As an indicator for apoptotic processes we measured protein expression levels of cleaved caspase 3 in all groups (Fig. 2A). While no changes were observed in LVs of KO mice, a 4-fold enhanced expression was detected in LVs of WT mice after 1 week of TAC. Similarly, mRNA levels of the fibrotic markers Fn-1 (Fig. 2B) and collagen type I and –III (Fig. 2C, D) were highly upregulated in WT mice. The measured values were associated with the expression levels of Sox9, which were upregulated at one week after TAC in WT mice and reached its expression maximum after two weeks (Fig. 2E, F). At 4 weeks after TAC Sox9 mRNA levels were back to its initial values. Contrary, upregulation of the fibrotic markers cannot be reported for KO mice until 4 weeks after TAC (Fig. 2B, C, D). Accordingly, Sox9 expression was only slight but non-significant upregulated after 4 weeks of pressure-overload (Fig. 2E, F). The observed association between expression levels of Sox9 and the fibrotic markers suggests Sox9 to be a trigger of these genes.

To underpin these findings, paraffin-embedded heart sections were stained for fibrosis (Fig. 3). A comparison confirmed an earlier initiation of hypertrophic processes combined with a strong fibrotic response starting already one week after TAC in WT mice while this onset of fibrosis seems to be delayed in the KO group. Furthermore, serial heart sections were stained for Sox9, the fibroblast-marker vimentin and the cardiomyocyte-marker troponin T2 to distinguish the source of Sox9 (Fig. 1; Supplementary material). In LVs of WT hearts Sox9 expression co-localized with vimentin as well as with troponin T2, indicating both, cardiac fibroblasts and cardiomyocytes as Sox9 producers. Contrary, in LVs of KO Sox9 expression was restricted vimentin-positive cells.

LV mRNA levels of Lox, an important mediator of collagen maturing, were measured and revealed to be highly upregulated in WT mice after one week of pressure overload (Fig. 2G). In LVs of KO mice no enhanced Lox expression was seen until 4 weeks after TAC.

Since myocardial remodeling is not only characterized by increased synthesis of new matrix proteins but also by increased degradation of existing matrix we analyzed the mRNA expression levels of Mmp2 (Fig. 2H). While the expression of Mmp2 was significantly increased in WT mice at one week after TAC, an upregulation in the KO group was not observed until 4 weeks after TAC, suggesting that not only the synthesis of new proteins but also the degradation of existing extracellular matrix are affected by the loss of cardiomyocyte-specific Sox9.

3.4. Ventricular function

The LV function was analyzed by echocardiography (Figs. 2 and 3; Supplementary material). LV ejection fraction (LVEF) as well as fractional shortening (FS) dropped in both groups at one week after TAC. Although not significant, WT mice appeared to have a slightly better performance after 2 and 4 weeks of TAC compared to KO mice. Simultaneously, the contractility of the left ventricle slightly declined as indicated by the LV inner diameter (LVID). The pressure-overload caused LV hypertrophic growth affecting the filling phase as well as ECM accumulation, stiffening the ventricle and impairing the systolic phase.

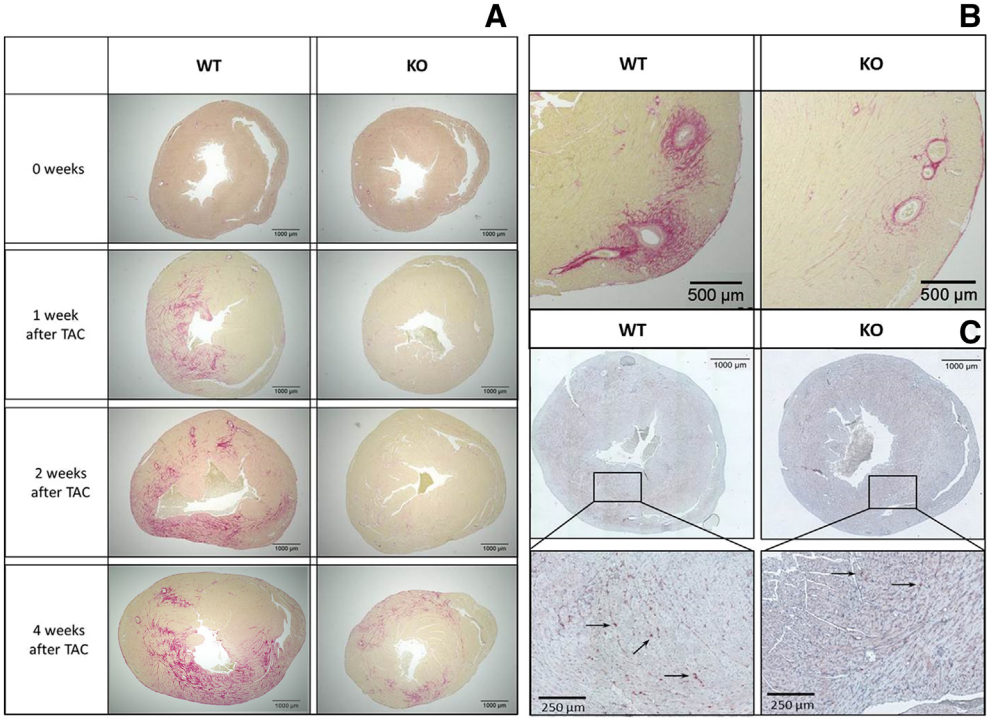

Fig. 3. Representative picro-sirius- and Sox9-stained heart sections of WT- and KO mice. A) Overview staining, B) typical left ventricular perivascular fibrosis due to pressure-overload (2 weeks of TAC) in WT mice. C) Representative Sox9 staining in WT and KO mice after two weeks of TAC. Arrows represent Sox9 in nuclei. KO mice show a diffuse cytoplasmic Sox9 signal with only few Sox9-positive nuclei. For serial staining of Sox9, vimentin and Troponin T2 see Fig. 1 of the Supplementary material.

4. Discussion

In the present study, we demonstrate for the first time the importance of cardiomyocyte-derived Sox9 on early stages of hypertrophic growth, fibrosis and remodeling in response to cardiac pressure-overload. We show that loss of cardiomyocyte-specific Sox9 ameliorates hypertrophic growth of the cardiomyocyte itself and suggest an influence on the response of neighboring cells, like cardiac fibroblasts, possibly by a cross-talk.

Sox9 plays a key role in chondrogenesis [9,10]. It is therefore not surprising that, during cardiac development, Sox9 is crucial for the correct formation of cardiac valves [12,13], which can be attributed to its cartilage-specific target genes [21,22]. Little is known about the role of Sox9 in adult mammalian cardiomyocytes, especially in response to pathophysiological stimuli, like cardiac injury or pressure-overload. In a recent study, Lacraz et al. presented Sox9 as a key regulator of cardiac fibrosis following myocardial infarction in a mouse model [18]. Using genome-wide RNA tomography and lineage-tracing they found Sox9 to be mainly active in the fibroblast population that repopulates the infarcted area after injury. Moreover, the enhanced Sox9 levels were correlated with the expression of collagen type I. In contrast, in the present study we used a cardiomyocyte-specific Sox9 knockout in order to estimate its cell-specific influence on the development and progression of LV hypertrophy and fibrosis.

4.1. Loss of Sox9 delays cardiac hypertrophy

Comparing basic physiological parameters prior to any intervention, Sox9 KO mice showed enhanced heart weights and slightly enhanced levels of hypertrophic markers and Sox9 compared to WT mice (Table 1). Since this phenotype is accompanied by a slight LV dilation, indicated by enlarged ventricle areas and a tendency of reduced ventricular function (Table 1), the observed basal hypertrophy might be a compensatory effect. Also, the tendency of elevated Sox9 expression, which seems paradox in a KO model, might be due to a compensating expression of Sox9 by non-cardiomyocytes as documented by immunohistochemistry (Fig. 1, Supplementary material). Controversially, pressure-overload did not further enhance hypertrophy in KO mice, but delayed its onset while hearts of WT mice were significantly hypertrophic after only one week of pressure-overload (Fig. 1). Accordingly, the LV expression of the hypertrophic markers was significantly upregulated after one week of TAC in WT mice but not until four weeks of pressure-overload in KO mice (Fig. 1C, F–K).

The cytokine Il-6 has been implicated in cardiovascular pathologies [23,24]. Melendez et al. observed concentric hypertrophy in rats after Il-6 infusion [25], and Zhao et al. report that deletion of Il-6 attenuated TAC-induced LV hypertrophy and ECM deposition in an Il-6$^{-/-}$ mouse model [3]. Accordingly, we observed highly increased Il-6 mRNA levels in WT mice after 1 week of pressure-overload (Fig. 1K) associated with hypertrophic growth and fibrosis. Il-6 is produced by cardiomyocytes and cardiac fibroblasts. In a murine model of angiotensin II-induced hypertrophy Ma et al. found macrophages to stimulate Il-6 expression in cardiac fibroblasts and proposed downstream activation of the Tgf-β-1/Smad3 pathway leading to cardiac fibrosis [26]. In adult mouse hearts TGF-β is localized in both the cardiomyocytes and the extracellular matrix [27] and has been shown to mediate cardiomyocyte growth, fibroblast activation and ECM deposition [28]. Although our KO affects only myocytes but not fibroblasts, both, Il-6- and Tgf-β expression were suppressed during the first weeks of pressure-overload (Fig. 1I–K). That's why we suggest cardiomyocyte-driven Sox9 as an upstream mediator of Il-6- and Tgf- β signaling leading to early hypertrophic growth and fibrosis (Fig. 4; Supplementary material).

4.2. Loss of Sox9 delays ECM deposition and collagen turnover

Enhanced collagen expression and –deposition are initially adaptive responses to myocardial pressure-overload, maintaining structural integrity and ventricular function. However, it promotes the stiffening of the myocardium, affecting both, mechanical contraction and relaxation and thus, leading to heart failure [29–31]. We observed highly enhanced expression levels of collagen type I, –III and Fn-1 after one and two weeks after TAC in LVs of WT mice (Fig. 2B–D). Contrary, KO mice did not show fibrotic changes until 4 weeks after TAC and even then, to a much lesser extent.

Besides cardiomyocytes, the dominating cardiac cell types include fibroblasts, vascular smooth muscle cells (VSMCs) and endothelial cells [32,33]. In general, cardiac fibroblasts are considered to be the main, although not the only producers of collagen in the heart [34,35]. Fibroblasts primarily express collagen type I and III while myocytes predominantly produce collagen type IV and VI [34,35]. Since our cardiomyocyte-specific Sox9 KO delayed the expression of collagen type I, -III and Fn-1, we suggest a Sox9-driven paracrine cross-talk promoting early structural changes in response to pressure-overload (Fig. 4; Supplementary material).

The progression of cardiac fibrosis is a highly dynamic process, including the expression but also the degradation of ECM. In the context of collagen turnover, matrix metalloproteinases (Mmp's) and their opponents, the Timp's (tissue inhibitors of metalloproteinases) play a key role [36–38]. In the healthy heart both enzymes are expressed in low levels but are strongly induced in the failing heart, predominantly expressed by fibroblasts [38-40]. Genetic loss of Mmp2 has been shown to preserve cardiac function during pressure-overload [41]. Other studies demonstrated enhanced Mmp2 expression in pressure-overloaded rat hearts [5,6]. This is in line with our findings of enhanced Mmp2 mRNA levels in LVs of WT mice after one week of pressure-overload (Fig. 2H). El Hajj et al. observed a link between Mmp2 and Lox, since enhanced Mmp2 levels were reduced by Lox inhibition in a rat model of volume overload-induced hypertrophy [4]. Moreover, Lox inhibition attenuated ventricular hypertrophy, blocked fibrosis and improved cardiac function [42]. These studies suggest Lox to be a key player in the progression of heart failure. In our study, Lox was significantly upregulated in WT mice (Fig. 2G) and was associated with Sox9 within the first two weeks of pressure-overload (Fig. 2E, F). Contrary, the deletion of Sox9 completely prevented Lox upregulation. These results suggest Lox to be a direct or indirect target gene of Sox9 (Fig. 4; Supplementary material). In turn, Sox9 might be a crucial activator of multiple adverse hypertrophic processes leading to maladaptive ECM remodeling and cardiac dysfunction.

4.3. Sox9 as mediator of a paracrine cross-talk?

The observed results suggest that cardiomyocyte-specific Sox9 not only affects target genes of the cardiomyocyte itself but, regarding fibrotic changes, also exerts paracrine effects via a cross talk with surrounding non-cardiomyocytes.

It has been shown, that cardiac fibroblasts and cardiomyocytes have an extensive and reciprocal communication via direct cell-cell interaction and soluble factors but also electrically [43,44]. Takeda et al. demonstrated that fibroblast-specific Krüppel-like factor (Klf5) is essential for the hypertrophic response of cardiomyocytes in a murine model of pressure-overload and suggests IGF-1 as paracrine mediator of hypertrophic growth [45]. Cardiac fibroblasts have been reported to secrete pro-inflammatory cytokines, including Il-1β, Il-6, TNFα and TGF-β, which directly leads to hypertrophic growth of cardiomyocytes [46–48]. Thum et al. reported, that silencing of fibrotic miR-21 did not only inhibit fibrosis but also reduced the growth of cardiomyocytes and cardiac dysfunction in a murine TAC model [49]. In turn, cardiomyocyte signaling triggers the proliferation, differentiation and ECM deposition of cardiac fibroblasts. Yuan et al. demonstrated that cardiomyocyte-derived miR-378 entered cardiac fibroblasts, thereby enabling a cross-talk between cardiomyocyte and fibroblast following pressure-overload and suppressing myocardial fibrosis [50].

In our study pressure-overload leaded to increased expression levels of collagen type I and –III as well as Fn-1 and Mmp2 in WT mice (Fig. 2B–D, H). All of these proteins are considered to be predominantly produced by cardiac fibroblasts [34,35]. Since no up-regulation of these proteins occurred in the KO group within the first weeks of pressure-overload, we suggest an influence of cardiomyocyte-specific Sox9 on the early response of cardiac fibroblasts, thus triggering differentiation and the accumulation of fibroblast-derived ECM and increasing the expression of Mmp2 (Fig. 4; Supplementary material). Future studies are warranted to analyze how cardiomyocyte-derived Sox9 signaling affects fibroblast-specific target genes.

4.4. Loss of Sox9 does not improve cardiac performance

Although the absence of Sox9 resulted in less hypertrophic growth and fibrosis/remodeling following TAC, it has not proven to be beneficial regarding the cardiac performance (Figs. 2 and 3; Supplementary material). Initial characterization revealed KO-hearts to be slightly hypertrophic, less contractile and with a dilative tendency. This might indicate a protective role of Sox9 in the healthy heart, since it seems to be involved in the maintenance of tissue structure and elastic properties of the heart.

In both groups pressure-overload caused a decline of LVEF, however, to a lesser extent in WT mice. Since lack of Sox9 inhibits the hypertrophic response following pressure-overload, WT mice seem to have a higher compensatory capacity, thus adapting better to pressure-overload than KO mice. Although the present study demonstrates a positive correlation between cardiomyocyte-driven Sox9 and hypertrophy-associated genes, its loss does not improve the cardiac performance.

To our knowledge, this is the first study demonstrating that cardiomyocyte-specific Sox9 mediates hypertrophic growth and ECM synthesis/accumulation in cardiac pressure-overload, thus crucially contributing to the remodeling of the left ventricle. We suggest that the presence of cardiomyocyte-derived Sox9 is essential for a variety of downstream processes following pressure-overload and that it affects not only the cardiomyocyte itself but also cardiac fibroblasts, possibly by a cross-talk.

4.5. Study limitation

Initially observed differences regarding the cardiac phenotype of both groups must be noted as a limitation to the study. However, since aortic banding did not enhance the initial differences but on the contrary, led to the opposite development with enhanced heart weights and elevated hypertrophy markers in the control group, we believe, that initial variations don't query the observed differences between both groups during pressure overload.

Supplementary data to this article can be found online at https://doi.org/10.1016/j.ijcard.2019.01.078.

Conflict of interest

The authors report no relationships that could be construed as a conflict of interest.

References

[1] T. Cornelius, S.R. Holmer, F.U. Muller, et al., Regulation of the rat atrial natriuretic peptide gene after acute imposition of left ventricular pressure overload, Hypertension 30 (1997) 1348–1355.
[2] T. Horio, T. Nishikimi, F. Yoshihara, et al., Inhibitory regulation of hypertrophy by endogenous atrial natriuretic peptide in cultured cardiac myocytes, Hypertension 35 (2000) 19–24.
[3] L. Zhao, G. Cheng, R. Jin, et al., Deletion of interleukin-6 attenuates pressure overload-induced left ventricular hypertrophy and dysfunction, Circ. Res. 118 (2016) 1918–1929.
[4] E.C. El Hajj, M.C. El Hajj, V.K. Ninh, et al., Inhibitor of lysyl oxidase improves cardiac function and the collagen/MMP profile in response to volume overload, Am. J. Physiol. Heart Circ. Physiol. 315 (2018) 463–473.
[5] J.T. Peterson, H. Hallak, L. Johnson, et al., Matrix metalloproteinase inhibition attenuates left ventricular remodeling and dysfunction in a rat model of progressive heart failure, Circulation 103 (2001) 2303–2309.
[6] Y. Sakata, K. Yamamoto, T. Mano, et al., Activation of matrix metalloproteinases precedes left ventricular remodeling in hypertensive heart failure rats: its inhibition as a primary effect of angiotensin-converting enzyme inhibitor, Circulation 109 (2004) 2143–2149.
[7] B. Lopez, A. Gonzalez, N. Hermida, et al., Role of lysyl oxidase in myocardial fibrosis: from basic science to clinical aspects, Am. J. Physiol. Heart Circ. Physiol. 299 (2010) H1–H9.
[8] P. Sivakumar, S. Gupta, S. Sarkar, et al., Upregulation of lysyl oxidase and MMPs during cardiac remodeling in human dilated cardiomyopathy, Mol. Cell. Biochem. 307 (2008) 159–167.
[9] L.J. Ng, S. Wheatley, G.E. Muscat, et al., SOX9 binds DNA, activates transcription, and coexpresses with type II collagen during chondrogenesis in the mouse, Dev. Biol. 183 (1997) 108–121.
[10] Q. Zhao, H. Eberspaecher, V. Lefebvre, et al., Parallel expression of Sox9 and Col2a1 in cells undergoing chondrogenesis, Dev. Dyn. 209 (1997) 377–386.
[11] H. Akiyama, M.C. Chaboissier, R.R. Behringer, et al., Essential role of Sox9 in the pathway that controls formation of cardiac valves and septa, Proc. Natl. Acad. Sci. U. S. A. 101 (2004) 6502–6507.
[12] V.C. Garside, R. Cullum, O. Alder, et al., SOX9 modulates the expression of key transcription factors required for heart valve development, Development 142 (2015) 4340–4350.
[13] J.A. Montero, B. Giron, H. Arrechedera, et al., Expression of Sox8, Sox9 and Sox10 in the developing valves and autonomic nerves of the embryonic heart, Mech. Dev. 118 (2002) 199–202.
[14] P. Li, H. Li, Y. Zheng, et al., Variants in the regulatory region of WNT5A reduced risk of cardiac conotruncal malformations in the Chinese population, Sci. Rep. 5 (13120) (2015).
[15] K. Amano, K. Hata, A. Sugita, et al., Sox9 family members negatively regulate maturation and calcification of chondrocytes through up-regulation of parathyroid hormone-related protein, Mol. Biol. Cell 20 (2009) 4541–4551.
[16] J.D. Peacock, A.K. Levay, D.B. Gillaspie, et al., Reduced sox9 function promotes heart valve calcification phenotypes in vivo, Circ. Res. 106 (2010) 712–719.
[17] J.D. Peacock, D.J. Huk, H.N. Ediriweera, et al., Sox9 transcriptionally represses Spp1 to prevent matrix mineralization in maturing heart valves and chondrocytes, PLoS One 6 (2011), e26769.
[18] G.P.A. Lacraz, J.P. Junker, M.M. Gladka, et al., Tomo-seq identifies SOX9 as a key regulator of cardiac fibrosis during ischemic injury, Circulation 136 (15) (2017) 1396–1409.
[19] O. Rahkonen, M. Savontaus, E. Abdelwahid, et al., Expression patterns of cartilage collagens and Sox9 during mouse heart development, Histochem. Cell Biol. 120 (2003) 103–110.
[20] H.A. Rockman, R.S. Ross, A.N. Harris, et al., Segregation of atrial-specific and inducible expression of an atrial natriuretic factor transgene in an in vivo murine model of cardiac hypertrophy, Proc. Natl. Acad. Sci. U. S. A. 88 (1991) 8277–8281.
[21] W. Bi, J.M. Deng, Z. Zhang, et al., Sox9 is required for cartilage formation, Nat. Genet. 22 (1999) 85–89.
[22] C. Healy, D. Uwanogho, P.T. Sharpe, Regulation and role of Sox9 in cartilage formation, Dev. Dyn. 215 (1999) 69–78.
[23] C.A. Hunter, S.A. Jones, IL-6 as a keystone cytokine in health and disease, Nat. Immunol. 16 (2015) 448–457.
[24] G.L. Kukielka, C.W. Smith, A.M. Manning, et al., Induction of interleukin-6 synthesis in the myocardium. Potential role in postreperfusion inflammatory injury, Circulation 92 (1995) 1866–1875.
[25] G.C. Melendez, J.L. McLarty, S.P. Levick, et al., Interleukin 6 mediates myocardial fibrosis, concentric hypertrophy, and diastolic dysfunction in rats, Hypertension 56 (2010) 225–231.
[26] F. Ma, Y. Li, L. Jia, et al., Macrophage-stimulated cardiac fibroblast production of IL-6 is essential for TGF beta/Smad activation and cardiac fibrosis induced by angiotensin II, PLoS One 7 (2012), e35144.
[27] N.L. Thompson, K.C. Flanders, J.M. Smith, et al., Expression of transforming growth factor-beta 1 in specific cells and tissues of adult and neonatal mice, J. Cell Biol. 108 (1989) 661–669.
[28] M. Bujak, N.G. Frangogiannis, The role of TGF-beta signaling in myocardial infarction and cardiac remodeling, Cardiovasc. Res. 74 (2007) 184–195.
[29] P. Camelliti, T.K. Borg, P. Kohl, Structural and functional characterisation of cardiac fibroblasts, Cardiovasc. Res. 65 (2005) 40–51.
[30] A.M. Segura, O.H. Frazier, L.M. Buja, Fibrosis and heart failure, Heart Fail. Rev. 19 (2014) 173–185.
[31] K.T. Weber, Targeting pathological remodeling: concepts of cardioprotection and reparation, Circulation 102 (2000) 1342–1345.
[32] I. Banerjee, J.W. Fuseler, R.L. Price, et al., Determination of cell types and numbers during cardiac development in the neonatal and adult rat and mouse, Am. J. Physiol. Heart Circ. Physiol. 293 (2007) H1883–H1891.
[33] A.R. Pinto, A. Ilinykh, M.J. Ivey, et al., Revisiting cardiac cellular composition, Circ. Res. 118 (2016) 400–409.
[34] S.L. Bowers, I. Banerjee, T.A. Baudino, The extracellular matrix: at the center of it all, J. Mol. Cell. Cardiol. 48 (2010) 474–482.
[35] S. Jane-Lise, S. Corda, C. Chassagne, et al., The extracellular matrix and the cytoskeleton in heart hypertrophy and failure, Heart Fail. Rev. 5 (2000) 239–250.

[36] E.C. El Hajj, M.C. El Hajj, V.K. Ninh, et al., Detrimental role of lysyl oxidase in cardiac remodeling, J. Mol. Cell. Cardiol. 109 (2017) 17–26.
[37] D. Fan, A. Takawale, J. Lee, et al., Cardiac fibroblasts, fibrosis and extracellular matrix remodeling in heart disease, Fibrogenesis Tissue Repair 5 (2012) 15.
[38] V. Polyakova, S. Hein, S. Kostin, et al., Matrix metalloproteinases and their tissue inhibitors in pressure-overloaded human myocardium during heart failure progression, J. Am. Coll. Cardiol. 44 (2004) 1609–1618.
[39] G. Sawicki, H. Leon, J. Sawicka, et al., Degradation of myosin light chain in isolated rat hearts subjected to ischemia-reperfusion injury: a new intracellular target for matrix metalloproteinase-2, Circulation 112 (2005) 544–552.
[40] W. Wang, C.J. Schulze, W.L. Suarez-Pinzon, et al., Intracellular action of matrix metalloproteinase-2 accounts for acute myocardial ischemia and reperfusion injury, Circulation 106 (2002) 1543–1549.
[41] H. Matsusaka, T. Ide, S. Matsushima, et al., Targeted deletion of matrix metalloproteinase 2 ameliorates myocardial remodeling in mice with chronic pressure overload, Hypertension 47 (2006) 711–717.
[42] J. Gonzalez-Santamaria, M. Villalba, O. Busnadiego, et al., Matrix cross-linking lysyl oxidases are induced in response to myocardial infarction and promote cardiac dysfunction, Cardiovasc. Res. 109 (2016) 67–78.
[43] Y. Feld, M. Melamed-Frank, I. Kehat, et al., Electrophysiological modulation of cardiomyocytic tissue by transfected fibroblasts expressing potassium channels: a novel strategy to manipulate excitability, Circulation 105 (2002) 522–529.
[44] R. Kakkar, R.T. Lee, Intramyocardial fibroblast myocyte communication, Circ. Res. 106 (2010) 47–57.
[45] N. Takeda, I. Manabe, Y. Uchino, et al., Cardiac fibroblasts are essential for the adaptive response of the murine heart to pressure overload, J. Clin. Invest. 120 (2010) 254–265.
[46] N. Takeda, I. Manabe, Cellular interplay between cardiomyocytes and nonmyocytes in cardiac remodeling, Int. J. Inflamm. 535241 (2011) 2011.
[47] N.A. Turner, Effects of interleukin-1 on cardiac fibroblast function: relevance to post-myocardial infarction remodelling, Vasc. Pharmacol. 60 (2014) 1–7.
[48] C. Vasquez, N. Benamer, G.E. Morley, The cardiac fibroblast: functional and electrophysiological considerations in healthy and diseased hearts, J. Cardiovasc. Pharmacol. 57 (2011) 380–388.
[49] T. Thum, Noncoding RNAs and myocardial fibrosis, Nat. Rev. Cardiol. 11 (2014) 655–663.
[50] J. Yuan, H. Liu, W. Gao, et al., MicroRNA-378 suppresses myocardial fibrosis through a paracrine mechanism at the early stage of cardiac hypertrophy following mechanical stress, Theranostics 8 (2018) 2565–2582.